# A BEM-based inverse algorithm to retrieve multi-dimensional heat transfer coefficients from transient temperature measurements

Alain J. Kassab[(1)], Eduardo Divo[(1)], and Mingking Chyu[(2)]
[(1)]*Department of Mechanical, Materials, and Aerospace Engineering, University of Central Florida, Orlando, Florida 32816-2450. Email: kassab@mail.ucf.edu.*
[(2)]*Mechanical Engineering, Carnegie Mellon University, Pittsburgh, PA 15213-3890. Email: mc47+@andrew.cmu.edu.*

## Abstract

We present a BEM-based inverse algorithm to retrieve multi-dimensional heat transfer coefficients ($h$) from surface temperature measurements. The time history of temperatures at convective BEM nodes is measured (or simulated). At each time level, a regularized least-squares functional is minimized to retrieve current fluxes and simultaneously smooth out temperature measurement errors. The regularization term weighs the square of deviations of BEM-computed fluxes from a mean flux to allow adjustment of temperatures and fluxes to obtain a "best fit" through noisy input data. Results for retrieval of $h$ over a square and a backward facing step show the 1-D approach fails to reproduce $h$, while our approach reproduces $h$ accurately while being robust to input errors.

## 1 Introduction

Non-intrusive techniques currently used to determine $h$ rely on certain physical principles to precisely determine surface temperature histories, and, in conjunction with theoretical assumptions, predict $h$ values. For instance, techniques relying on temperature dependent characteristic color changes of liquid crystals and the more recent laser induced fluorescence

based method[1] both use the analytical solution for the surface temperature $\theta(t)= (T(t) - T_i) / (T_\infty - T_i)$ of a semi-infinite medium

$$\theta(t) = 1 - exp(h^2 t/k\rho c) erfc[\, h(t/k\rho c)^{\frac{1}{2}}] \qquad (1)$$

initially at temperature $T_i$ and impulsively subjected to convection with the surroundings at temperature $T_\infty$, to model surface temperature histories and to predict $h$ values: once $\theta(t)$ is measured, Eqn. (1) is solved for $h$. This approach leads to erroneous values of $h$, in particular, in regions such as corners, stagnation points of impinging jets, and downstream of film cooling holes of turbine blades where heat transfer cannot be modeled as 1-D for any duration of time. It is herein proposed to use the BEM to resolve 2D and 3D heat transfer and determine $h$ by inverse methods. The BEM is ideally suited for this inverse problem as surface temperatures and fluxes appear as nodal unknowns. These are precisely the variables required in inverse analysis. Surface fluxes have been retrieved using BEM-based inverse algorithms and internal temperature measurements, see Kurpisz and Nowak[2]. In a numerical study, Maillet *et al.*[3] formulate an inverse BEM-based approach to retrieve angular distributions of $h$ from a cylinder using second order regularization to stabilize results. Hsieh and Farid[4] use an inverse BEM approach to retrieve the angular variation of $h$ over a rough heated horizontal cylinder in an experiment where steady-state surface temperatures are measured non-intrusively by infrared scanning. Martin and Dulikravich[5] use a steady-state BEM-based approach in a numerical study to retrieve $h$ and Singular Value Decomposition to stabilize results. However, transient surface temperature measurements are more commonly used in experiments, and we develop a BEM-based inverse algorithm to retrieve multi-dimensional varying $h$ from transient surface temperature measurements. At each time level, a regularized functional is minimized to retrieve current heat fluxes and simultaneously smooth out the effect of measurement errors. Results presented for 2-D retrieval of $h$ over a square and a backward facing step show that the 1-D approach fails to reproduce correct $h$ values, while our inverse approach reproduces $h$ accurately and is robust to input errors.

# 2 BEM solution of the Diffusion Equation

At each time of interest, solution of the inverse problem requires the temperature distribution which is governed by the heat diffusion equation. This is solved using the BEM and the time marching convolution scheme

detailed in Brebbia, Telles, and Wrobel[6]. In this method, boundary temperatures at time level $F$ are related to boundary fluxes at that time and all previous times by

$$[\hat{H}]^{FF}\{T\}^F - [G]^{FF}\{q\}^F = \sum_{p=1}^{F-1}\left([G]^{Fp}\{q\}^p - [H]^{Fp}\{T\}^p\right) \qquad (2)$$

The influence matrices $H$ and $G$ are $N$x$N$ matrices, where $N$ is the number of boundary nodes used to discretize the geometry, and they are evaluated numerically[6]. The matrix $[\hat{H}]^{FF} = [H]^{FF} - \frac{1}{2}\rho c[I]$, with $[I]$ as the identity matrix. The right-hand-side of Eqn. (2) contains convolution information and can be collapsed into a simple vector $\{c\}^F$, while the left-hand-side can be re-ordered according to boundary conditions to obtain $[A]\{x\}^F = \{b\}^F$, which is solved by direct or iterative methods.

# 3 Inverse Problem Definition and Functional Regularization

Film coefficient modeling is actually a direct problem since time history temperature measurements are used to impose first kind boundary conditions at convective boundaries, while fluxes are directly solved using the BEM. However, small measurement errors in input temperatures translate into large deviations of computed heat fluxes and, consequently, erroneous $h$ values. To mitigate this problem, the retrieval of $h$ is treated as an inverse problem, and a regularized objective function, $Z^F$, to be minimized, is defined at each time level, $F$, as

$$Z^F = \sum_{i}^{NB}[(\hat{T}_i^F - T_i^F)/\Delta T^F]^2 + \beta\sum_{i}^{NB}[(q_i^F - \overline{q}_i^F)/\Delta q^F]^2 \qquad (3)$$

where $NB$ is the number of boundary nodes at which convective boundary conditions are imposed, $\hat{T}_i^F$ are measured temperatures at convective boundary(ies), $T_i^F$ are BEM-computed temperatures to be optimized by minimizing the functional, and $\Delta T^F$ is the maximum range of temperatures in the medium at time level, $F$. The regularization parameter, $\beta$, is tuned to damp out oscillations, $q_i^F$ are optimized heat fluxes, $\overline{q}_i^F$ is an interpolation of heat fluxes, and $\Delta q^F$ is the maximum range of heat fluxes at time level $F$. Regularization allows the minimization process to find a "best fit" of temperatures and fluxes, given noisy data, and the

regularization parameter, $\beta$, plays a most important role in controlling solution smoothing while preventing large deviations from measured temperatures. The term $\overline{q}_i^F$ is not used in traditional regularization, where heat fluxes are usually regularized with respect to zero. Subtracting $\overline{q}_i^F$ allows optimized heat fluxes $q_i^F$ to approach $\overline{q}_i^F$ as the regularization parameter $\beta$ approaches infinity, and optimized temperatures $T_i^F$ to approach measurements $\hat{T}_i^F$ as $\beta$ approaches zero. The $\overline{q}_i^F$ are found by interpolation of heat fluxes at convective surfaces and is represented symbolically by the linear relation,

$$\overline{q}_i^F = A_{ik}\, q_k^F \tag{4}$$

The interpolant matrix $A_{ik}$ can be derived through least-square fitting of approximating polynomials. Introducing the above into $Z^F$ yields,

$$Z^F = \sum_{i=1}^{NB} [(\hat{T}_i^F - T_i^F)/\Delta T^F]^2 + \beta \sum_{i=1}^{NB} [(B_{ik}\, q_k^F)/\Delta q^F]^2 \tag{5}$$

where the matrix $B_{ik} = \delta_{ik} - A_{ik}$, and $\delta_{ik}$ is the Krönecker delta. Minimizing the above functional directly by differentiating with respect to $q_j^F$ and setting the result to zero leads to,

$$X_{ij}\left(\hat{T}_i^F - T_i^F\right) = m^F \beta\, C_{jk}\, q_k^F \tag{6}$$

where $X_{ij} = \partial T_i^F / \partial q_j^F$ is the sensitivity matrix, $m^F = \left(\Delta T^F / \Delta q^F\right)^2$, and $C_{jk} = B_{ik} B_{ij}$. The temperatures and fluxes are related by re-casting the discretized BIE as,

$$T_i^F = \overline{H}_{ik}^{FF} G_{kj}^{FF} q_j^F + d_i^F \tag{7}$$

where, $\overline{H}_{ik}^{FF}$ is the inverse of $\hat{H}_{ik}^{FF}$ and $d_i^F = \overline{H}_{ik}^{FF} c_k^F$. From this expression, the sensitivity matrix can be easily identified as, $X_{ij} = \partial T_i^F / \partial q_j^F = \overline{H}_{ik}^{FF} G_{kj}^{FF}$. Introducing Eqn. (7) leads to

$$X_{ij}\left(\hat{T}_i^F - X_{ik} q_k^F - d_i^F\right) = m^F \beta\, C_{jk}\, q_k^F \tag{8}$$

and rearranging and solving for $q_k^F$ finally leads to

$$\left(X_{ij} X_{ik} + m^F \beta\, C_{jk}\right) q_k^F = X_{ij}\left(\hat{T}_i^F - d_i^F\right) \tag{9}$$

This algebraic set can be solved by direct or indirect methods at each time level to obtain optimized boundary fluxes. After heat fluxes are obtained, Eqn. (7) is used to calculate optimized boundary temperatures. It is important to point out that when performing the matrix product $X_{ij}X_{ik}$, the indices $i$ and $j$ take on values of those boundary elements at which inverse convective conditions are imposed, while $k$ takes on values, $k = 1, ..., N$. The rest of the indices in Eqn. (9) take on values of those elements where inverse convective conditions are applied. The algebraic system in Eqn. (9) should be augmented to size $N$ to obtain a square system.

# 4 Numerical Implementation

Numerical solution of the boundary integral equation for the diffusion equation follows standard BEM, Brebbia *el al*[6]. Gram-Schmidt orthogonalization is used to obtain a polynomial curve-fit and to determine the interpolation matrix $A_{ik}$. A homogeneous parameter $\eta$ is introduced to define a 1-D parametrization of the convective boundary. However, as sharp corners are usually encountered on such boundaries and preclude smooth transformation, independent interpolations are performed along piecewise smooth sections, and then arranged together to form the final matrix $A_{ik}$. Figure (1) illustrates the curve-fitting process along a cornered boundary. Determining the interpolation matrix for boundary heat fluxes is automated by checking the angle between adjacent elements. When an angle $\gamma$ is detected to differ from 180° by a fixed value $\Delta\gamma$ (in this case fixed to 30°), a new independent curve-fit is performed. Polynomial representation of fluxes along each straight segment is taken as

$$\overline{q}\ (\eta) = \sum_{n=0}^{N} c_n\, p_n(\eta) \tag{10}$$

where Gram-Schmidt polynomials $p_n(x)$ have the following form,

$$p_{j+1}(\eta) = (\eta - \alpha_{j+1})p_j(\eta) - \beta_j\, p_{j-1}(\eta),\ \ p_0(\eta) = 1,\ \ p_{-1}(\eta) = 0 \tag{11}$$

and the coefficients $\alpha$ and $\beta$ are,

$$\alpha_{k+1} = \sum_{i=1}^{n} \eta_i [p_k(\eta_i)]^2 \Big/ \sum_{i=1}^{n} [p_k(\eta_i)]^2\ ,\ \ \beta_k = \sum_{i=1}^{n} [p_k(\eta_i)]^2 \Big/ \sum_{i=1}^{n} [p_{k-1}(\eta_i)]^2 \tag{12}$$

where the $\eta_i$'s correspond to the location of boundary nodes along the interpolation path ( $-1 < \eta < 1$). The order of polynomials used in the code varies between three and five depending directly on the number of boundary nodes along the interpolation path. A least-squares cofactor matrix is constructed as,

$$d_{lm} = \sum_{i=1}^{n} p_l(\eta_i) p_m(\eta_i) \tag{13}$$

which is diagonal due to orthogonality of the polynomials $p_l$ over the points $\eta_i$. Therefore, interpolated heat fluxes along the path are,

$$\overline{q}_{\ i} = p_l(\eta_i) d_{lm}^{-1} p_m(\eta_k)\ q_k \tag{14}$$

From the previous expression, the interpolation matrix $A_{ik}$ is identified as,

$$A_{ik} = p_l(\eta_i) d_{lm}^{-1} p_m(\eta_k) \tag{15}$$

for $i$ and $k$ corresponding to elements along the current straight interpolation path. This can be extended to piecewise smooth curves.

# 5 Examples

A set of numerical examples is presented to validate developments above. A square region and a backward facing step geometry are considered.

## 5.1. Square Region Under Convection

We first consider a square region subject to convection at the top and right surfaces and insulated at the bottom and left surfaces, see Fig. (2). The exact solution is derived as,

$$\frac{T(x,y,t) - T_{amb}}{T_{ini} - T_{amb}} = \sum_{n=0}^{\infty} \sum_{m=0}^{\infty} A_{n,m} \frac{cos(\alpha_n x) cos(\beta_m y)}{cos(\alpha_n L) cos(\beta_m L)} e^{-\frac{k\lambda_{n,m}^2 t}{\rho c}} \tag{16}$$

where $A_{n,m}$=$4H^2/[L(\alpha_n^2 + H^2) + H][L(\beta_m^2 + H^2) + H]$ and $H = h/k$. Eigenvalues satisfy: $\alpha_n tan\alpha_n L = H$, $\alpha_n = \beta_m$, and $\lambda_{n,m}^2 = \alpha_n^2 + \beta_m^2$. Properties of pure Aluminum are used: $k = 2.37 W/cmK, c = 903 J/Kg$ and $\rho = 0.002702 Kg/cm^3$. The initial condition is set to $T_{ini} = 30°C$, the ambient temperature is $T_{amb} = 800°C$, and $h = 0.04 W/cm^2 K$. The square is $L = 5cm$ on a side.

Equation (16) is used to simulate measurements at convective nodes, and the 1-D approximation in Eqn. (1) is used to retrieve $h$. This is compared with the exact $h$ along nodes 11 to 30 in Fig. (3.a-b) after 1 and 10 seconds respectively. Clearly, the 1-D predicted $h$ is inaccurate with errors reaching as much as 50%, even at short times. Next, Eqn. (16) is used to simulate measurements for the BEM-based inverse algorithm with random errors of $\pm 0.5°C$ and $\pm 1°C$ added to simulate expected noisy input data (a maximum of $\pm 1°C$ is expected) and to investigate effectiveness of the regularization term. In Fig. (4.a-b), $h$ is retrieved without regularization ($\beta = 0$) after 1s and 10s respectively. Amplification of input noise in retrieved $h$ values is apparent. Damping of these errors is achieved by selecting an effective regularization parameter, $\beta$, whose value is problem dependent: the higher the input error, the more damping is required, and $\beta$ also exhibits geometry dependence. In this paper, the selected linear relationship between the standard deviation of input errors, $\sigma$, and $\beta$, with the constant of proportionality set to 5, provides excellent damping in all cases. A linear relation between $\beta$ and $\sigma$ is commonly used in functional regularization; however, the value of $\beta$ is usually taken to be very small ($10^{-1} - 10^{-4}$), as heat fluxes are traditionally regularized with respect to zero. Assuming a 99% confidence level, $\sigma = |\text{max random error}|/2.576$, and $\sigma$ is taken as constant over time. Fig. (5.a-b) shows retrieved $h$ values with $\beta = 5\sigma$ and reveals oscillations in $h$ completely damped down, a considerable improvement over non-regularized solutions.

### 5.2. Backward Facing Step Under Convection

A backward-facing step geometry is considered next, see Fig. (6) for geometry and boundary conditions. Thermophysical properties of pure Aluminum are again used. The initial condition is set to $T_{ini} = 30°C$, and the ambient temperature is $T_{amb} = 800°C$. The irregular geometry precludes analytical solution, and the direct problem is solved using the BEM with 60 equally spaced quadratic subparametric elements. The temperature history at convective nodes provided by the direct BEM solution is used as input data to simulate measurements. The imposed $h$ grows exponentially between $h = 0.01W/cm^2K$ at node 26 to $h = 0.074W/cm^2K$ at node 40, and decreases exponentially from $h = 0.055W/cm^2K$ at node 41 to $h = 0.0075W/cm^2K$ at node 45. This distribution simulates a maximum at the re-entry corner. Twenty time levels are equally distributed between 0 and 20s for the convolution

scheme. Next, in the inverse problem, in order to retrieve $h$ BEM-computed boundary temperatures at convective nodes are used as input to force time-dependent boundary conditions. In Fig. (7.a-b), the 1-D approximation of $h$ is compared with exact values along nodes 26 to 45 after 1s and 20s. Next, the BEM-based inverse approach is used with random errors of $\pm 0.5°C$ and $\pm 1°C$ added to the input surface temperatures. Results for $h$ predicted with $\beta = 0$ are shown in Fig. (8.a-b) for 1s and 20s respectively and for $\beta = 5\sigma$ in Fig. (9.a-b). Results reveal that the regularized inverse approach retrieves $h$ faithfully.

# 6 References

1 Bizzak, D.J. and Chyu, M.K., "Use of laser-induced fluorescence thermal imaging system for local jet impingement heat transfer measurements," *Int. J. Heat and Mass Transfer,* Vol. 38, No. 2, pp. 267-274, 1995.

2 Kurpisz, K. and Nowak, A.J., "BEM approach to inverse heat conduction problems," *Eng. Analysis*, Vol. 10, pp. 291-297, 1992.

3 Maillet, D., Degiovanni, A., and Pasquetti, R., "Inverse Heat Conduction Applied to the Measurements of Heat Transfer Coefficient on a Cylinder: Comparison Between an Analytical and a Boundary Element Technique," *J. Heat Transfer,* Vol. 113, pp. 549-557, 1991.

4 Farid, M.S. and Hsieh, C.K., "Measurement of the free convection heat transfer coefficient for a rough horizontal nonisothermal cylinder in ambient air by infrared scanning," *J. Heat Transfer*, Vol. 114, pp. 1054-1056, 1992.

5 Martin, T.J. and Dulikravich, G.S., "Inverse Determination of Steady Heat Convection Coefficient Distributions," *J. Heat Transfer,* Vol. 120, pp. 328-334, 1998.

6 Brebbia, CA., Telles, J.C.F., and Wrobel, L., *Boundary Element Techniques in Engineering,* Spinger-Verlag, New York, 1985.

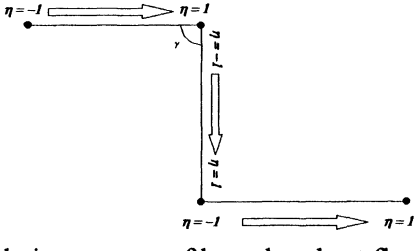


Figure 1: Interpolation process of boundary heat fluxes.

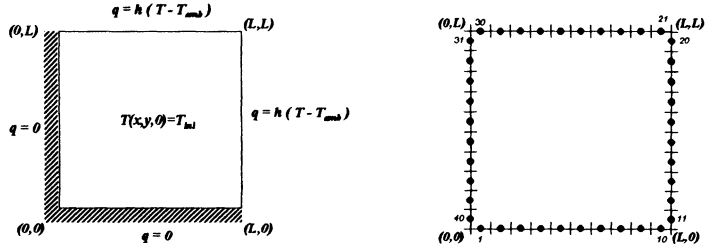


Figure 2: Geometry, boundary and initial conditions, and BEM mesh.

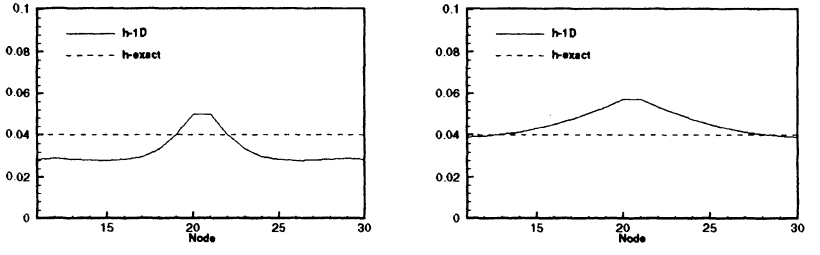


(a) (b)

Figure 3: Comparison of 1-D and exact $h$ after: (a) 1s and (b) 10s.

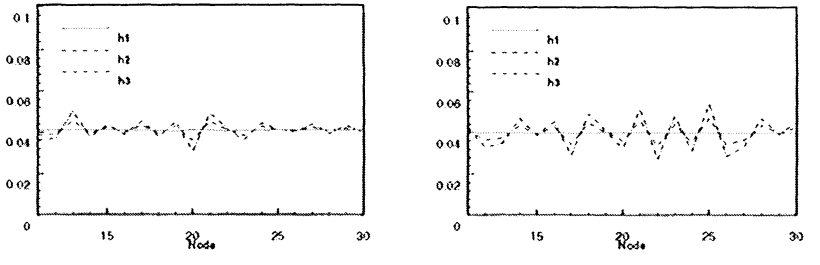


(a) (b)

Figure 4: BEM retrieved $h$ at: (a) 1s and (b) 10s. Input errors: h1:$\pm 0$°C, h2:$\pm 0.5$°C, and h3:$\pm 1$°C. Regularization parameter: $\beta = 0$.

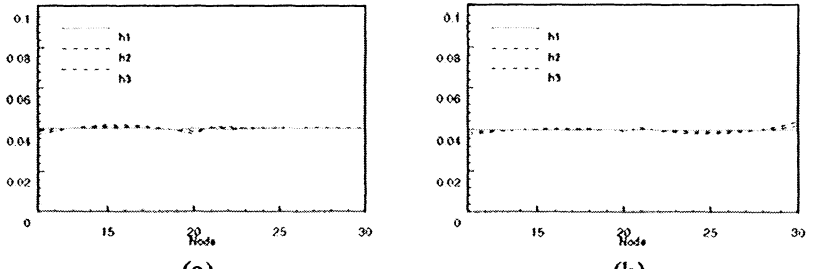


(a) (b)

Figure 5: BEM retrieved $h$ at: (a) 1s and (b) 10s. Input errors: h1:$\pm 0$°C, h2:$\pm 0.5$°C, h3:$\pm 1$°C. Regularization parameter: $\beta = 5\sigma$.

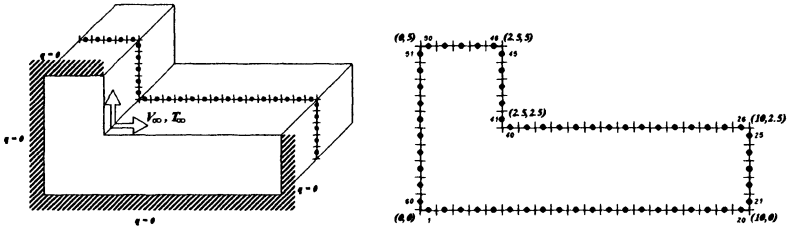

Figure 6: Geometry, boundary conditions, and BEM discretization.

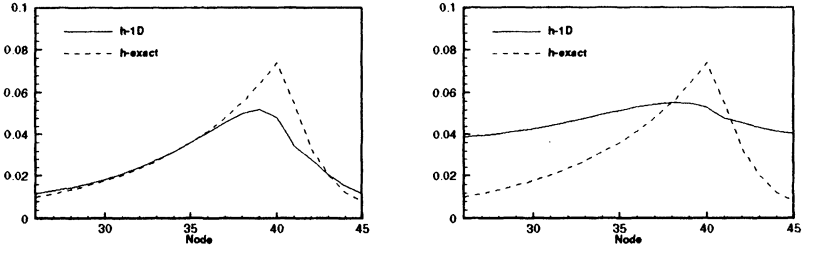


(a) (b)

Figure 7: Comparison of 1-D and exact $h$ after (a) 1s and (b) 10s.

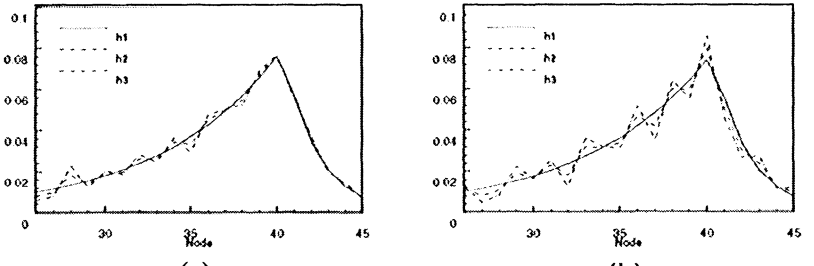


(a) (b)

Figure 8: BEM retrieved $h$ at: (a) 1s and (b) 10s. Input errors: h1:$\pm$0°C, h2:$\pm$0.5°C, h3:$\pm$1°C. Regularization parameter: $\beta = 0$.

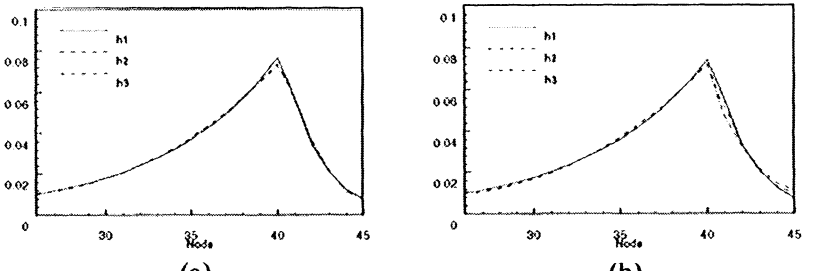


(a) (b)

Figure 9: BEM retrieved $h$ at: (a) 1s and (b) 10s. Input errors: h1:$\pm$0°C, h2:$\pm$0.5°C, h3:$\pm$1°C. Regularization parameter: $\beta = 5\sigma$.